

# Engineering a Universal Dengue Virus Vaccine using a Virus-Like Particle Scaffold

Danielle A. Basore<sup>1,3</sup>, Carolyn M. Barcellona<sup>2</sup>, Thomas B. Jordan<sup>1,4</sup>, Donna E. Crone<sup>1</sup>, Sharon Isern<sup>2</sup>, Scott F. Michael<sup>2</sup>, Christopher Bystroff<sup>1</sup>

<sup>1</sup>Biological Sciences, Rensselaer Polytechnic Institute, Troy, NY, USA, <sup>2</sup>Biological Sciences, Florida Gulf Coast University, Fort Myers, FL, USA, <sup>3</sup>Mercy College, Dobbs Ferry, NY, USA. <sup>4</sup>Charles River Labs, Wilmington MA, USA.

## Abstract

The fusion loop (FL), a 51-residue segment of the dengue virus (DENV) envelope (E) protein, has been shown to bind antibodies that neutralize DENV infection in cell culture. Vaccination with this loop could raise broadly neutralizing antibodies and avoid antibody dependent enhancement in second serotype infections associated with whole virus vaccination. We propose a new DENV vaccine in which FL has been genetically fused to a well-known and highly immunogenic carrier, the human papillomavirus (HPV) L1 protein (L1). Chimeric L1-FL was expressed in human cell culture, but expression levels of virus-like particles (VLP) were initially low. Expression levels were improved after adding a bridging disulfide bond at the base of the loop, and were further improved by transfecting cells with a mixture of 9 parts chimera to 1 part wild-type L1 expression vectors. VLPs formed from the chimeric construct were purified using ultracentrifugation and were shown to form hollow particles of the expected size using transmission electron microscopy. The improvements in expression are discussed in the context of a theoretical pathway for folding and assembly of VLPs.

## 1 | INTRODUCTION

Viruses affect all domains of life, and so many organisms have evolved mechanisms to detect and respond to viral capsids<sup>1-3</sup>. In vertebrates these mechanisms, including activation of toll-like receptor 4<sup>4</sup>, size selective entrance into the germinal centers of the lymph nodes<sup>5</sup>, and recognition of the highly multivalent structure that enhances avidity to the maturing B-cells<sup>6</sup>, all make viral capsids efficient immunogens.

Human papilloma virus (HPV) L1 protein self-assembles into highly stable T=7 icosahedral 55 nm VLPs, identical in structure to the natural HPV capsid<sup>7,8</sup>. The VLPs each consist of 360 copies of L1, arranged in 72 pentamers, called capsomeres, which contain no other DNA or protein and are stabilized by multiple internal and inter-unit disulfide bonds. Because HPV infection is associated with the development of certain cancers, L1 VLPs are widely used as anti-cervical cancer vaccines<sup>9</sup>.

L1 can fold and form VLPs despite mutations in certain surface exposed loops. Specifically, up to 39 residues of HPV L2 protein have been inserted at position 137 (DE loop) in L1 of HPV Type 16, without disrupting VLP formation or stability<sup>10</sup>. The HPV L1 monomer has a greek key or jelly roll fold, with a well-studied, theoretical folding pathway that provides guidance when considering the effect on folding of inserted antigenic loops<sup>11-14</sup>. One loop in particular, called the DE loop is predicted to fold late in the monomeric folding pathway, explaining the tolerance for insertions at this location<sup>15</sup>. The ability to genetically insert peptide antigens into HPV L1 VLPs provides an opportunity to use the immunogenicity of VLPs to create multifunctional vaccines and focus immunity toward neutralizing epitopes by inserting specific sequences into L1<sup>16</sup>.

DENV is a tropical virus spread primarily by two mosquito vectors, *Aedes aegypti* and *Aedes albopictus*. Climate change and globalization have spread the vectors, and therefore the virus, whose clinical manifestations range from mild flu-like symptoms, rash, and joint pain, to dengue hemorrhagic fever (DHF) or dengue shock syndrome (DSS). Exposure to any one of DENV's four known serotypes does not provide cross-protective immunity to the other three. On the contrary, infection with a second serotype can result in the very severe conditions DHF and DSS through the process of antibody dependent enhancement (ADE) of infection, a phenomenon that occurs when antibodies from the first infection bind weakly to the viral particles of the second serotype, and target the still infectious viral particle to

51 macrophages and other Fc receptor-bearing cells that are normally not infected<sup>17</sup>. A global estimate from  
52 the WHO estimates 390 million DENV infections, half a million hospitalizations and approximately 12,500  
53 deaths annually, making dengue one of the most prevalent vector-borne diseases in the world<sup>18</sup>. While  
54 there is a tetravalent vaccine available for dengue, it uses the full-length DENV envelope (E) surface protein  
55 and elicits an enhancing antibody response that can result in more severe outcomes in naïve recipients when  
56 they are exposed to DENV<sup>19</sup>. Consequently, use of this vaccine has been discontinued in many countries  
57 or is only licensed for use in people older than nine who have already experienced one or more DENV  
58 infections. The development of a safer dengue vaccine that does not induce enhanced disease is a high  
59 priority.

60 A subunit vaccine that focuses immunity specifically against neutralizing epitopes of DENV may  
61 avoid vaccine-induced ADE. A broadly neutralizing epitope has been identified by localizing the binding  
62 sites of broadly neutralizing monoclonal antibodies derived from patients post-DENV infection<sup>20</sup>. These  
63 antibodies blocked the fusion of the virus with the endosomal membrane within the infected cell, severing  
64 the life cycle of the virus<sup>21</sup>. The antibody binding is conformationally dependent and negatively affected by  
65 mutations within the neutralizing epitope, confirming that the neutralizing antibodies bound to that site.  
66 The neutralizing epitope encompasses the part of domain II of the envelope (E) protein of DENV, referred  
67 to as the fusion loop (FL), which is highly conserved. During infection, the DENV E protein undergoes a  
68 dramatic conformational change upon exposure to low pH, visible in TEM images<sup>22</sup>, producing a trimeric  
69 spike that exposes the hydrophobic FL and triggers fusion between the viral and endosomal membranes<sup>20</sup>.  
70 However, designing such a subunit vaccine is not trivial. Here we demonstrate proof of principle of the  
71 protein design elements of a hypothetical vaccine candidate by inserting the DENV FL into an exposed  
72 loop of HPV L1, creating a chimeric VLP containing parts from two antigenic proteins from different  
73 viruses. Considerable further work would be required to ascertain if these VLPs could induce a useful  
74 immune response.

## 75 **2 | RESULTS**

### 76 **2.1 | Design of constructs**

77 Two different chimeric proteins were designed and produced. In both, two adjacent HPV L1 residues,  
78 A137 and N138 in the DE loop were removed to create space and replaced with DENV E protein residues.  
79 In the initial chimera (designated FL), the DENV FL insert consisted of a 55 amino acid consensus from  
80 the four serotypes of DENV, flanked on each side with a glycine residue to allow flexibility. The second  
81 chimera was designed by modeling experiments using the crystal structures of HPV 16 L1 (PDB id 2R5H)  
82 and DENV serotype 2 E protein (PDBid 1OAN, Accession AHB63923). This approach resulted in the  
83 insertion of 51 amino acids from DENV serotype 2 E protein, flanked by upstream CGP and downstream  
84 GPC motifs, creating a new potential disulfide at the base of the DENV E insert. This second chimera was  
85 designated cysFL to reflect the design of the cysteine disulfide at the base of the DENV E insert. CGP/GPC  
86 linkers have been used to stabilize the display of short peptides on the surface of the enzyme thioredoxin  
87 on the surface of bacteria for the purpose of high throughput screening<sup>23</sup>. By adding CGP/GPC to the  
88 interface between the L1 and the FL insert, we encourage the formation of a disulfide bond that produces  
89 topological isolation (i.e., “pinching” off) of the FL insert. This decreases the effect of the additional loop  
90 entropy and encourages the proper folding of both the L1 monomer and FL insert<sup>24</sup>. The pair of flexible  
91 Gly-Pro dipeptides is believed to isolate, to some extent, the folding of the FL from the folding of L1,  
92 making both more efficient. Amino acid sequences of both chimeras and a model for the resulting structure  
93 are shown in Figure 1.

### 94 **2.2 | Expression of recombinant proteins**

95 The expression of the constructs was confirmed by Western blot analysis of equal amounts of the denatured  
96 cell lysates of each transfection probed with CAMVIR-1 anti-HPV L1 Ab (Figure 2). The wild type L1  
97 band can be seen at approximately 55 kDa. The chimeric L1 bands, L1-FL or L1-cysFL, are slightly higher  
98 at approximately 61 kDa, because of the inserts. L1-FL expression was only one tenth of the level of L1-  
99 WT, indicating that this chimera is less stable than the WT L1 protein. The expression of the CGP/GPC FL  
100

101 construct, L1-cysFL, was approximately 3-fold higher than for L1-FL, indicating that this chimera showed  
102 increased stability compared to the initial L1-FL construct, but was still somewhat less stable than WT.

103

### 104 **2.3 | Confirmation of L1-FL expression in the cytoplasm**

105 Images of transfected 293TT cells provide visual confirmation of expression of GFP in green (Figure 5).  
106 Red fluorescence shows L1 protein expression bound to CAMVIR-1 anti-HPV L1 antibody. Overlapping  
107 fluorescence (orange) indicates that both GFP and L1 proteins are expressed in the same cell, although this  
108 does not always occur because the plasmid has separate promoters. Peri-nuclear L1 fluorescence shows that  
109 the L1 protein remains in the cells and not in the supernatant. Binding was not observed with the  
110 conformationally sensitive anti-FL monoclonal antibody 1.6D<sup>20</sup> with either the L1-FL or L1-cysFL  
111 constructs, possibly due to the chimeric FL not being folded correctly in the cytoplasm because the disulfide  
112 bonds have not yet formed.

### 113 **2.4 | Characterization of assembled VLPs by ultracentrifugation**

114 Rate zonal ultracentrifugation conditions were selected to discriminate between unassembled, assembled  
115 and aggregated L1 proteins in equal amounts of cell lysates. Following centrifugation, nine equal volume  
116 fractions were collected from the bottom to the top of the centrifuge tube and assayed by Western blot.  
117 VLPs appear in the middle fractions (2-8), while fraction 1 consists of aggregates that sediment to the  
118 bottom of the tube and fraction 9 is unassembled monomers or capsomeres that do not enter the gradient.  
119 Results of these experiments are shown in Figure 3. Wild type HPV L1 (L1-WT) VLPs sediment to fractions  
120 4 - 6, suggesting that they form uniformly sized particles. L1-FL enters the gradient but appears in equally  
121 low quantity in all fractions with no discernable peak, indicating that assembly of these particles is reduced  
122 and is not uniform. L1-cysFL VLPs express and assemble better overall than the uncrosslinked counterpart  
123 and sediment mostly to fractions 6 and 7, corresponding to a uniform but less dense VLP than the wild type,  
124 likely due to the increased hydrodynamic diameter of the particles with the addition of the inserted FL.

125 Additional transfection experiments were performed to investigate if co-expression of a small  
126 amount (1:9) of WT L1 could rescue the expression and assembly of the chimeric L1-FL and L1-cysFL  
127 proteins. Western blot analysis showed that expression and VLP formation are improved for both L1-FL  
128 and L1-cysFL in the presence of WT L1. Interestingly, the ratio of L1-FL to L1-WT in these middle  
129 fractions is approximately 1:1, even though 9:1 of plasmid was transfected, indicating that even in the  
130 presence of WT L1, L1-FL has reduced stability and may be degraded or aggregate. Co-expression of WT  
131 L1 appears to stabilize and promote assembly of the L1-cysFL VLPs to near WT levels.

### 132 **2.5 | Analysis of VLPs by transmission electron microscopy**

133 Wild type HPV 16 particles produced by expression of L1 in HEK 293TT cells and purified by  
134 ultracentrifugation are visible with uranyl acetate staining (Figure 4). They are roughly spherical and  
135 approximately 55nm across, indicating properly folded protein and assembled particles. Additionally,  
136 purchased HPV 18 L1 particles also appear similar to HPV 16 L1 VLPs. The chimeric L1-cysFL samples  
137 display hollow 55 nm spheres but without clear capsomere segmentation. We speculate that the FLs, being  
138 much larger than the native DE loop, obscure the capsomere boundaries. We were not able to observe VLPs  
139 of the L1-FL chimera by TEM.

### 140 **2.6 | Confirmation of correctly folded and accessible DENV FL in VLPs**

141 An ELISA was used to probe chimeric, assembled VLPs for correctly folded DENV FL (Figure 6). High  
142 bind 96 well plates were coated with VLPs and probed with a conformationally-sensitive human anti-  
143 DENV FL Ab (1.6D), followed by goat anti-human IgG HRP. Increasing concentrations of hMAb 1.6D  
144 bind specifically to L1-cysFL VLPs in a dose-dependent manner, but not to WT VLPs. This indicates that  
145 the FL in chimeric L1-cysFL VLPs is properly folded, exposed, and accessible to an anti-DENV FL  
146 antibody when bracketed by the CGP/GPC motif.

147

## 148 **3 | DISCUSSION AND CONCLUSIONS**

149 The challenge in expressing a chimeric VLP is that success depends on spontaneous protein self-  
150 organization at multiple distinct levels, capsid monomer folding, pentamer (capsomere) formation from  
151 monomers, formation of the super-quaternary structure of the icosahedral particle from capsomeres and

152 folding of the insert, any of which may be disrupted by the fusion of the different viral proteins. Our initial  
153 attempt utilizing a DENV FL sequence flanked by glycines (L1-FL) did not express at high levels and did  
154 not assemble efficiently into VLPs. An inserted loop could produce this result via two likely mechanisms-  
155 entropic effects in folding or steric effects in oligomerization. An entropic barrier to folding may have been  
156 introduced when the DENV FL was inserted into the L1 DE loop, increasing the contact order<sup>25</sup> of that loop  
157 and possibly slowing its folding. The results are consistent with a FL whose folding is controlled by free  
158 energy and which, because of its smaller size, folds much faster than L1. We pursued two different  
159 strategies to overcome this limitation: redesign of the FL insert site and coexpression with a small amount  
160 of WT L1. Both strategies were successful in stabilizing the chimeric protein and improving assembly of  
161 chimeric VLPs.

162 As viral structural proteins, HPV L1 and DENV FL are both heavily disulfide crosslinked for  
163 stability. We reasoned that the presence of an additional disulfide at the base of the FL insertion site might  
164 effectively lock the FL in its folded state and separate it's folding from L1. We propose that the designed  
165 covalent crosslink in L1-cysFT returns the L1 DE loop conformational entropy to its approximate wild-  
166 type value, allowing L1 to fold at its native rate or at a more native-like rate. Molecular modeling did not  
167 show steric interference between FL and L1, despite the 51-residue size of the FL in the L1-cysFL construct.  
168 Experimental results showed that bracketing the FL insert with a disulfide containing CGP/GPC motif  
169 improved expression and VLP assembly.

170 Coexpression of defective monomers can often poison the structure and function of multimeric  
171 proteins (the dominant negative effect). Conversely, coexpression of functional monomers of a multimer  
172 can often rescue partially defective monomers. We used this reasoning and coexpressed a small amount of  
173 WT L1 along with each of the chimeric constructs. We hypothesized that these wild type monomers would  
174 relieve steric stress and encourage proper folding and assembly of VLPs. Molecular dynamics simulations  
175 done as a supplement to this work seems to suggest that this is the case, with one wild type monomer being  
176 included per pentamer, and allowing particle assembly to proceed (see supplemental information). VLP  
177 assembly of both of the chimeras was improved by coexpression with WT L1, which preferentially  
178 coassembled into the VLPs in a ratio higher than the ratio of coexpression. The migration of these mixed  
179 VLPs during rate zonal ultracentrifugation was shifted towards the bottom of the gradient, similar to WT  
180 VLPs, probably due to the particles having fewer monomeric units with a FL insert.

181 The chimeric HPV L1/DENV FL proteins described here self-assemble into VLPs that are  
182 potentially attractive multi-pathogen vaccine candidates. For DENV in particular, the focus on a broadly  
183 neutralizing epitope may help to solve the problem with ADE faced by current vaccines. We also show  
184 two different methods that are useful for stabilizing expression and assembly of chimeric proteins: Design  
185 of flanking sequences that can form a disulfide bond to isolate the inserted sequence from the host protein  
186 was shown to improve VLP formation. Coexpression with WT L1 resulted in formation of higher levels  
187 of mixed VLPs that still contained chimeric monomers. This work extends the successful combination of  
188 vaccines, such as the MMR and DTaP, in an effort to produce vaccines that can be provided at lower cost  
189 to generate coverage against multiple pathogens in a single dose.

## 191 **4 | MATERIALS AND METHODS**

### 192 **4.1 | Design of constructs**

193 Multiple HPV-L1 sequence alignments were carried out in UGENE<sup>26</sup> using MUSCLE<sup>27</sup>. Structures were  
194 inspected and homology models were constructed using MOE (Molecular Operating Environment, CCG,  
195 Montreal). Manual docking was used to position the FL (PDBid 1OAN residues 67-117) in relation to a  
196 model of the HPV-L1 capsomere (PDBid 2R5K), followed by loop building using MOE's Loop Modeler  
197 function and local energy minimization. The flanking sequences CGP/GPC were added in such a way that  
198 the two cysteines were within 6Å and could form a disulfide bond. Genes for all designed constructs were  
199 made by Genscript (New Jersey), using the p16L1-GFP plasmid which co-expresses HPV type 16 L1 and  
200 GFP<sup>28</sup>.

### 201 **4.2 | Cell culture and transfection**

202 Human embryonic kidney HEK 293TT cells (ATTC, Manassas, VA) were cultured in Dulbecco's Modified  
203 Eagle Medium (DMEM) supplemented with 10% (v/v) FBS, 2 mM Glutamax, 100 U/mL penicillin G, 100  
204 µg/mL streptomycin, 0.25 µg/mL amphotericin B, and 250 µg/mL hygromycin B at 37°C with 5% (v/v)  
205 CO<sub>2</sub>. Cells were transfected in serum free DMEM using Mirus TransIT-293 transfection reagent (Mirus  
206 #MIR 2704) according to manufacturer's protocol and incubated at 37°C with 5% (v/v) CO<sub>2</sub> for 4 days.  
207 GFP fluorescence was first observed ~48 h post-transfection. Cells were harvested and spun in a clinical  
208 centrifuge at 700 rpm for 15 min at 4°C. Cell pellets were re-suspended in 500 µL 2x lysis buffer consisting  
209 of 1/10 volume 10% (v/v) Triton X-100, 1/20 volume 1 M ammonium sulfate adjusted to pH 9.0, and 1:500  
210 dilution of Pierce Universal Nuclease for Cell Lysis (Thermo Scientific #88700) in phosphate buffered  
211 saline (PBS).

#### 212 **4.3 | Immunofluorescence and confocal microscopy**

213 Confocal microscopy was performed as previously described<sup>20</sup>. HEK 293TT cells were grown until 25%  
214 confluent on no. 1.5 Gold Seal coverglass coverslips (Erie Scientific, Portsmouth, NH, USA) in each well  
215 of a 6-well plate (Corning, Kennebunk, ME, USA) in complete DMEM without hygromycin. Cells were  
216 transfected with plasmids (Genscript, Piscataway, NJ, USA) containing a GFP-expressing reporter gene  
217 using Mirus TransIT-293 transfection reagent (Mirus Bio, Madison, WI, USA) and incubated at 37°C with  
218 5% (v/v) CO<sub>2</sub> for 4 days. Cells were fixed in Formalde-Fresh Solution (ThermoFisher) for 1h at RT and  
219 permeabilized with 70% (v/v) ethanol for 30 min at RT, rinsing between each step with PBS. Transfected  
220 cells were immunostained and incubated overnight at RT with a primary Ab solution containing 2 µg/mL  
221 of either anti-HPV16 L1 mouse monoclonal IgG<sub>2a</sub> Ab CAMVIR-1 (Santa Cruz Biotechnology, Dallas, TX)  
222 or anti-DENV hMAb 1.6D<sup>20</sup> in 0.1% (v/v) Tween20 (Sigma-Aldrich, St. Louis, MO), 5% (w/v) non-fat dry  
223 milk, and PBS. Secondary Ab solution consisting of 2 µg/mL Alexa Fluor 594-conjugated goat anti-mouse  
224 or goat anti-human IgG (H+L) (Invitrogen, Carlsbad, CA) in 0.1% Tween20 and PBS was added and  
225 incubated overnight at RT. Nuclei were counterstained with 0.5 µg/mL Hoechst (Cambrex, Walkersville,  
226 MD) for 15 min at RT followed by a final rinse step. Fluoromount-G (Southern Biotech, Birmingham, AL)  
227 was used to mount coverslips onto Fisherbrand Superfrost microscope slides (Fisher Scientific, Pittsburgh,  
228 PA). Images were obtained using an Olympus FV1000 Confocal Microscope System.

#### 229 **4.4 | Maturation and purification of VLPs**

230 Cell lysate was matured by 18-24 hours incubation in a 37°C water bath and clarified by incubation for 10  
231 min on ice followed by the addition of 0.17 volumes of 5M NaCl (85µL/500µL lysate). This solution was  
232 spun at 5,000 xg for 10 min at 4°C to pellet debris. The supernatant was transferred to a new 1.5mL tube  
233 and spun again.

#### 234 **4.5 | Ultracentrifugation of VLPs**

235 Rate-zonal density gradients were prepared using 60% Optiprep (Sigma #D1556-250ML). 10% and 30%  
236 solutions were prepared in Dulbecco's phosphate-buffered saline (DPBS)/0.8M NaCl. Gradients were  
237 created using inclined rotation (Gradient Mate, BioComp) in ultracentrifuge tubes (Beckman #349622).  
238 125µL of clarified lysate was added to the top of each gradient tube. Tubes were then spun in an SW50  
239 rotor at 45,000 RPM for 30 min at 20°C. Nine fractions (~525µL each) were collected from the bottom of  
240 each tube using a Beckman Fraction Recovery System.

#### 241 **4.5 | HPV L1 SDS-PAGE and Western blots**

242 2-20% precast gels (Biorad) were used for running SDS-PAGE. Samples were prepared by diluting 1:1 in  
243 Laemmli buffer with DTT and boiling for 10 minutes. Before loading onto the gel, samples were spun for  
244 1 minute at 10,000 RPM in an Eppendorf microfuge. Gels were run at 100V for 1 hour and 15 minutes in  
245 Tris-Glycine-SDS running buffer. Proteins were transferred to a PVDF membrane at 0.3 amps for 1  
246 h 15 min. The membrane was blocked with PBS-T + 3% BSA for 1h at room temperature. Primary  
247 anti-HPV 16 L1 antibody (CAMVIR-1, Santa Cruz Biotechnology, Dallas, TX ) was added to the  
248 membrane diluted 1:500 in PBS-T + 3% BSA and incubated overnight at 4°C. The membrane  
249 was then washed for 30 min with PBS-T, followed by secondary antibody (Alexafluor 488 goat  
250 anti-mouse) diluted 1:500 in PBS-T at room temperature for 3 h 30 min. The membrane was  
251 washed again with PBS-T for 30 min at RT, then dried overnight before scanning.

252 **4.6 | DENV FL enzyme linked immunoassay**

253 Corning brand high-bind 96-well plates (ThermoFisher, Waltham, MA) were coated with 100  $\mu$ L/well of  
254 antigen, either L1-WT VLP or L1-cysFL VLP. Plates were incubated at 4°C for 48 h, equilibrated to  
255 room temperature, then rinsed 6x with wash buffer containing 0.5% (v/v) Tween20 (Sigma) in PBS.  
256 Wells were blocked with 200  $\mu$ L blocking buffer containing 5% (w/v) non-fat dry milk and 0.5% (v/v)  
257 Tween20 in PBS, incubated at RT for 1 h, and rinsed 6x with wash buffer. Varying concentrations of  
258 primary anti-DENV FL HMAb 1.6D (REFS 19, 20 Costin, Schieffelin) were prepared in wash buffer, 100  
259  $\mu$ L/well was added and incubated at RT for 1 h 30 min, then rinsed 6x with wash buffer warmed to 37°C.  
260 Secondary peroxidase-conjugated affinity purified goat anti-human IgG (Pierce, Rockford, IL, USA) was  
261 diluted to 2  $\mu$ g/mL in wash buffer, 100  $\mu$ L/well was added and incubated covered at RT for 1 h. After a  
262 final 37°C wash step, color was developed with tetramethylbenzidine peroxide (ProMega, Madison, WI).  
263 The reaction was stopped after 3 min by adding 1M phosphoric acid (Sigma, Saint Louis, MO), and the  
264 absorbance was read at 450 nm.

265 **4.7 | Electron microscopy**

266 The VLP fraction collected by ultracentrifugation was desalted by centrifugal filter (Centriprep 30K,  
267 Millipore Sigma) to remove Optiprep. 0.5  $\mu$ L of the desalted VLP fraction was air dried onto a 300 mesh  
268 Carbon Type B copper grid (Ted Pella, Redding CA), for approximately 10 minutes, then stained with 0.5  
269  $\mu$ L 2% uranyl acetate solution for 60 s. Excess stain was blotted away gently. Images were collected using  
270 a JEOL 2011 TEM with an accelerating voltage of 200 kV. Images were taken at a nominal magnification  
271 of 100,000x.

272  
273 **SUPPLEMENTARY MATERIALS**

274 The following are provided for additional depth. Supplementary Figure 1. Multiple sequence alignment and  
275 phylogram for 23 mutually diverse primate papilloma virus L1 sequences, showing sites of high variability.  
276 Supplementary Figure 2. An illustration of greek-key, jelly roll protein folding pathway and assembly of  
277 the capsomeres and VLPs, showing loop intercalation. Supplementary Figure 3. Blow-up image of the  
278 modeled cysFL insertion, near the 5-fold axis of the capsomere. Supplementary Figure 4. Relative staining  
279 of HPVL1-WT and HPVL1-FL by conformational antibodies to the FL. Supplementary Figure 5. Wild-  
280 type HPVL1 tetramer. Supplementary Figure 6. HPVL1-cysFL tetramer. Supplementary Video 1.  
281 Molecular dynamics simulation of the wild-type HPVL1 tetramer. Supplementary Video 2. Molecular  
282 dynamics simulation of the HPVL1-cysFL tetrameric state.

283  
284 **ACKNOWLEDGEMENTS**

285 The Authors declare that there is no conflict of interest. This work was supported by NIH  
286 R01GM099827-01A1 to CB and SFM. We would like to express our thanks to John Schiller for helpful  
287 discussions and the HPV L1 expression system.

288  
289 **AUTHOR CONTRIBUTIONS**

290 Danielle A. Basore: Data curation; investigation; methodology; validation; visualization; writing-original  
291 draft; writing-review and editing.

292 Carolyn M. Barcellona: Data curation; investigation; methodology; validation; visualization; writing-  
293 original draft; writing-review and editing.

294 Thomas B. Jordan: Data curation; investigation; methodology; validation; visualization; writing-review  
295 and editing.

296 Donna E. Crone: Methodology; validation; writing-review and editing.

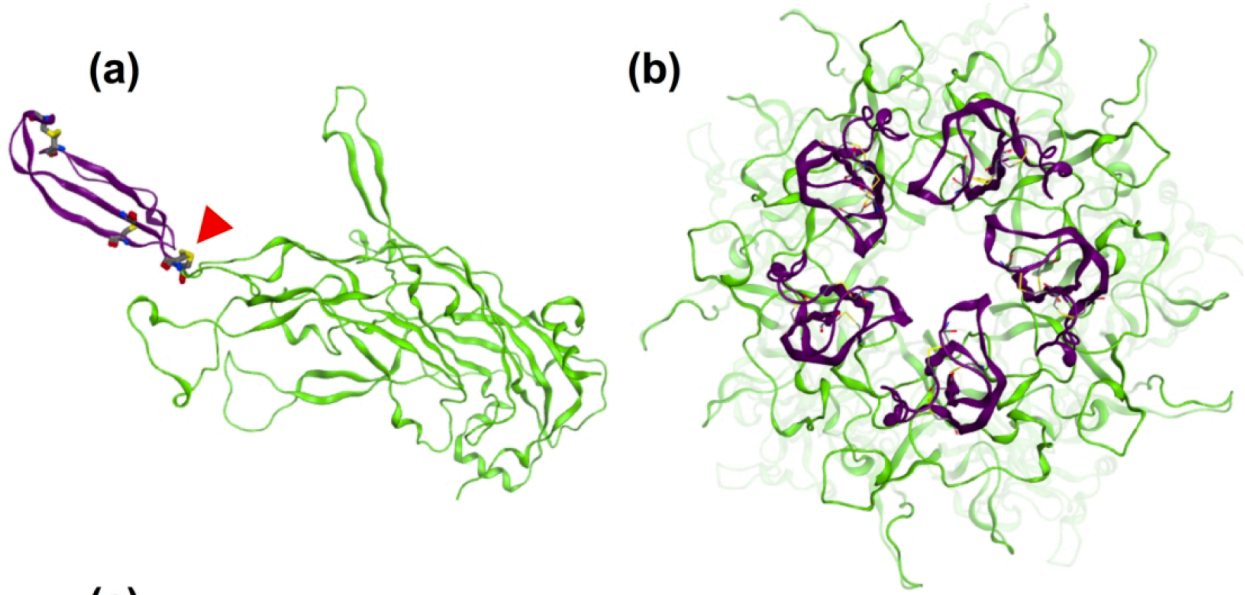
297 Christopher Bystroff: Conceptualization; data curation; investigation; methodology; project  
298 administration; validation; visualization; writing-original draft; writing-review and editing.

299 Scott F. Michael: Conceptualization; data curation; methodology; project administration;  
300 validation; visualization; writing-original draft; writing-review and editing

301

302

303 **FIGURE 1** (a) Design of 558-residue HPV16-L1 chimeras with inserted 58-residue DENV FL sequences  
 304 inserted into the DE loop, replacing Ala-Asn (red). The cysFL insert contains flanking CGP/GPC motif for  
 305 improved stability (green), while FL has a single Gly. Native disulfide-forming cysteines are shaded (cyan,  
 306 intramolecular; yellow, intermolecular) (b) Modeled structure of chimeric HPV16 L1 monomer and  
 307 capsomere, based on crystal structures of HPV11-L1 (PDBid:2R5K) and DENV2 E-protein  
 308 (PDBid:3C5X), showing the FL or cysFL in black.  
 309  
 310



(c) HPV16 L1

```
MSLWLPSEATVYLPPVPVSKVVSTDEYVARTNIYYHAGTSRLLAVGHYPYFPIKKPNNK
ILVPKVSGLQYRVFRIHLDPNKFPGFDPDTSFYNPDTQRLVWACVGVGVGRGQPLGVGIS
GHPLLNLKDDTENASAYAANAGVDNRECISMDYKQTQLCLIGCKPPIGEHWGKGSPECTN
VAVNPGDCPPLELINTVIQDGMVDTGFGAMDFTTLQANKSEVPLDICTSICKYPDYIK
MVSEPYGDSLFFYLRRQMFVRHLFNRAAGTVGENVPDDLYIKGSGSTANLASSNYFPTP
SGSMVTSDAQIFNKPYWLQRAQGHNNGICWGNQLFVTVDVTRSTNMSLCAAISTSETT
YKNTNFKEYLRHGEEYDLQFIFQLCKITLTADVMTYIHSMNSTILEDWNFGLQPPPGGT
LEDTYRFVTSQAIACQKHTPPAPKEDPLKKYTFWEVNLKEKFSADLDQFPLGRKFLLQA
GLKAKPKFTLGKRKATPTTSSTSTTAKRKRKL
```

DENV inserts

FL

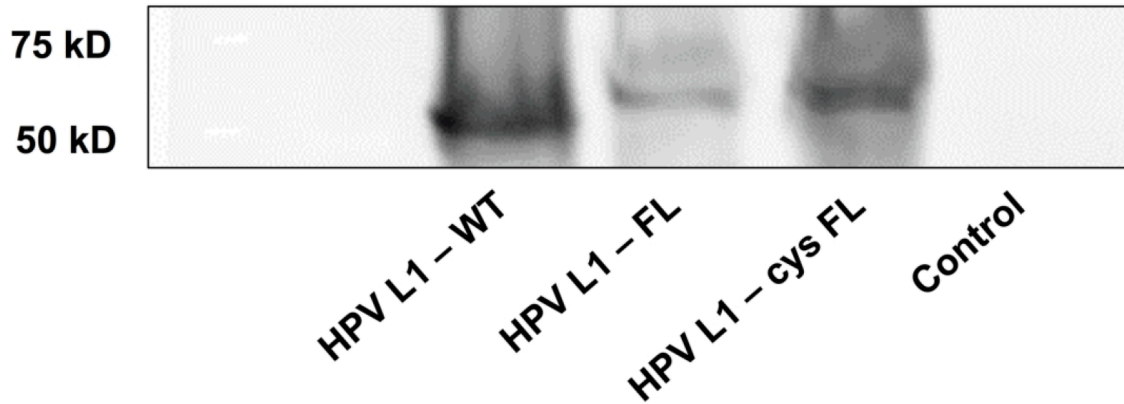
```
ITNTTDSRCPTQGEPTLNEEQDQNFVCKHTMVDRGWGNGCGLFGKGGIVTCAMFC
```

cysFL

```
CGPNTTTSRCPTQGEPTLNEEQDKRFVCKHSMVDRGWGNGCGLFGKGGIVTCAGPC
```

311  
 312

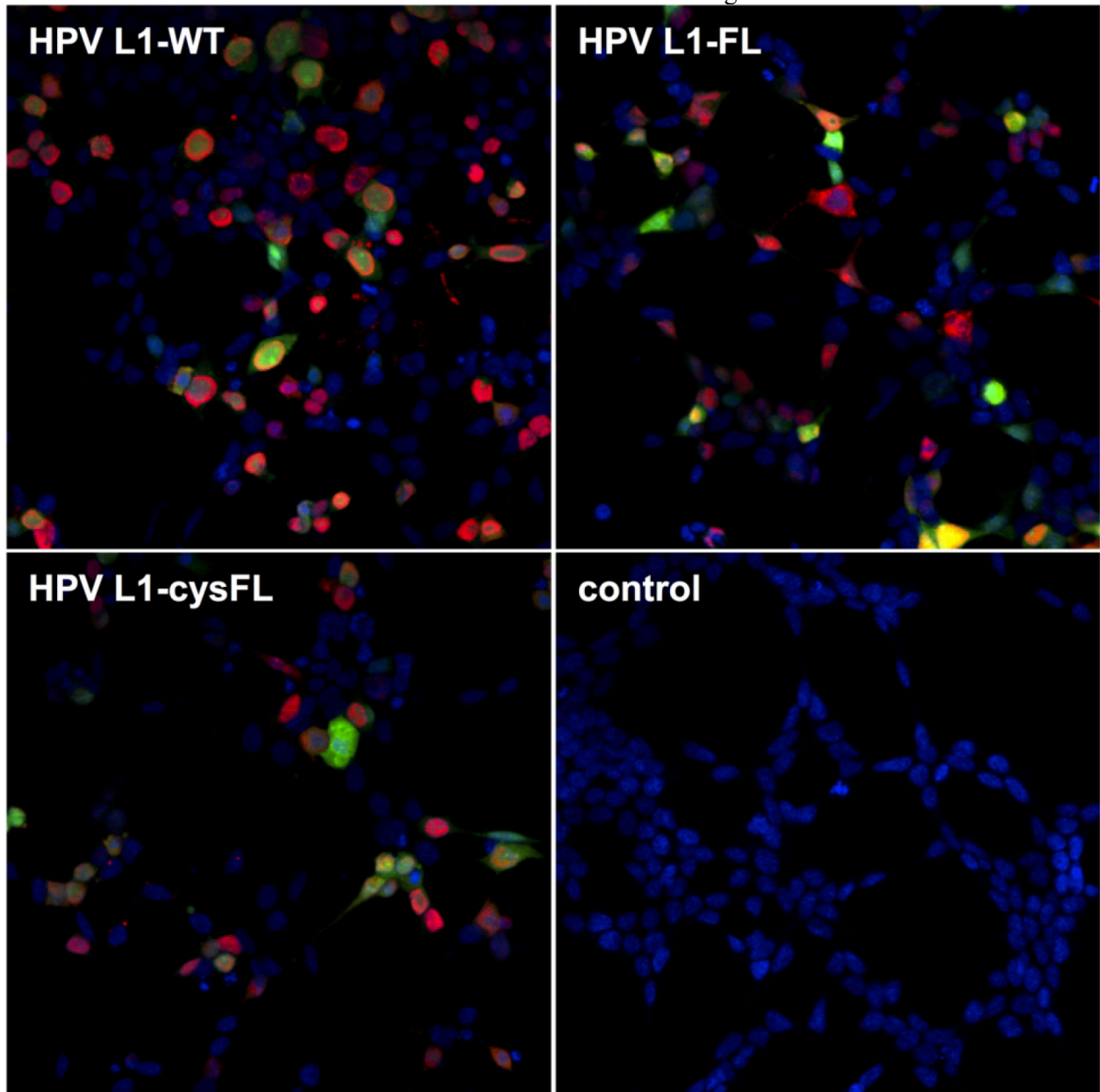
313 **FIGURE 2** Expression of chimeric proteins in transfected cells. Western blot of relative expression levels  
314 of wild type HPV16 L1 and the two chimeric constructs with a consensus DENV FL and with a DENV2  
315 FL and a cysteine disulfide lock (cysFL). The L1 protein is detected using an anti-L1 mouse monoclonal  
316 Ab. Untransfected cell lysate is run as a negative control. 50 and 75 kD size standards are indicated. WT  
317 L1 is expressed at a higher level than either chimera. The chimeric L1 proteins are slightly larger than the  
318 WT protein.



319  
320

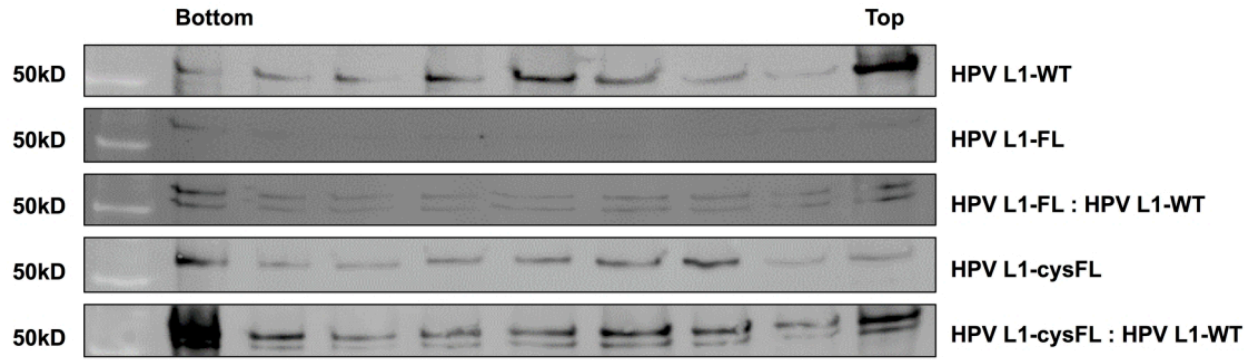


321 **FIGURE 3** Immunofluorescence microscopy of transfected cells (400X magnification). L1 protein (red) is  
322 detected using an anti-L1 mouse monoclonal Ab. GFP (green) is co-expressed from the transfected plasmid.  
323 Nuclei are counterstained blue. Untransfected cells are shown as a negative control.



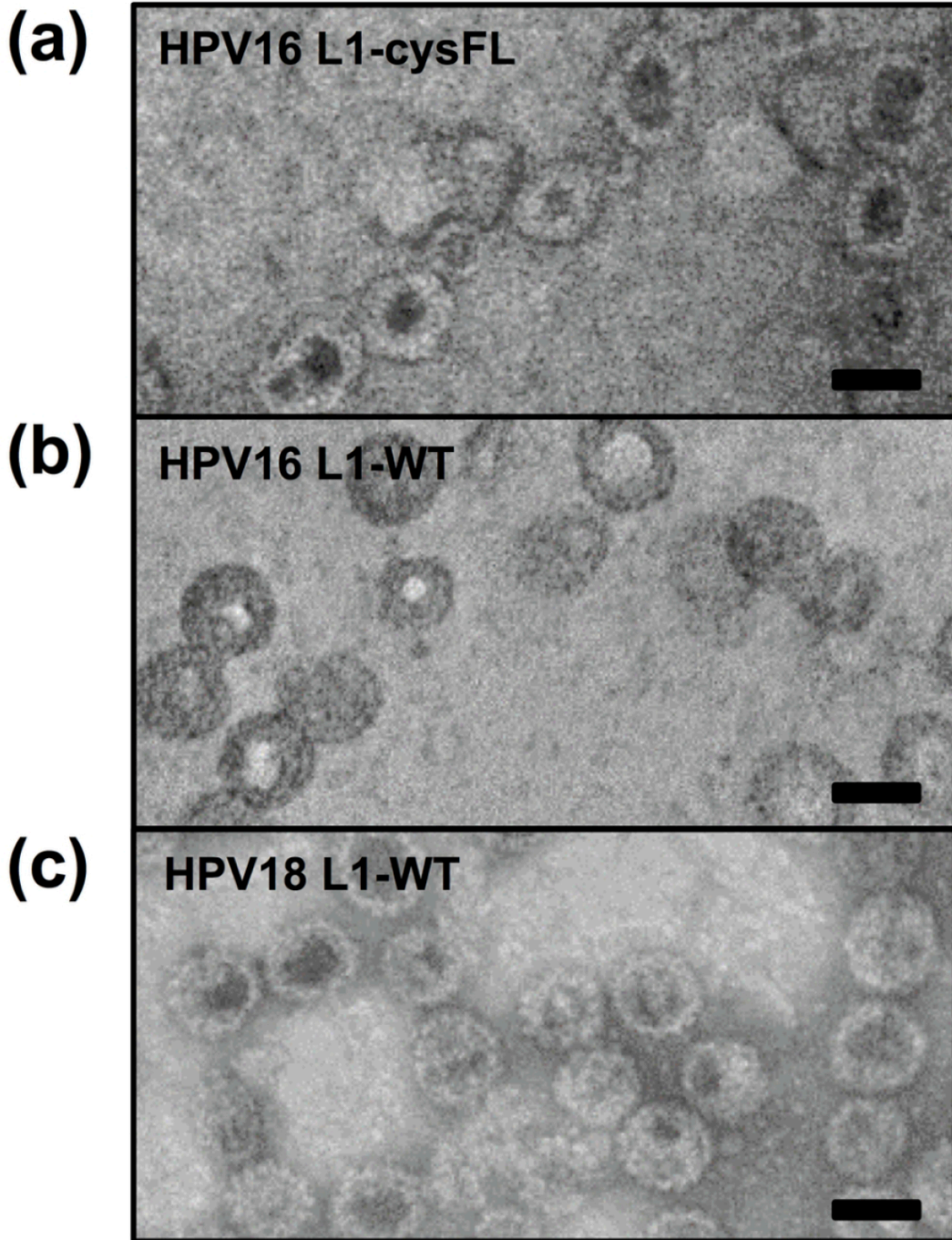
324  
325

326 **FIGURE 4** Assembly of chimeric virus like particles. Western blots of fractions from rate zonal  
327 centrifugation of matured, transfected cell lysates. WT L1, the consensus FL and the DENV2 FL with the  
328 disulfide (cysFL) were compared. Additionally, matured lysates from cell transfected with a 9:1 ratio of  
329 chimeric to WT L1 were compared to evaluate the ability of WT L1 to rescue assembly of chimeras. The  
330 L1 protein is detected using an anti-L1 mouse monoclonal Ab. 50 kD size standards are indicated.  
331 Assembled VLPs migrate into the center fractions. The chimeric L1 proteins are slightly larger than the  
332 WT L1 protein.



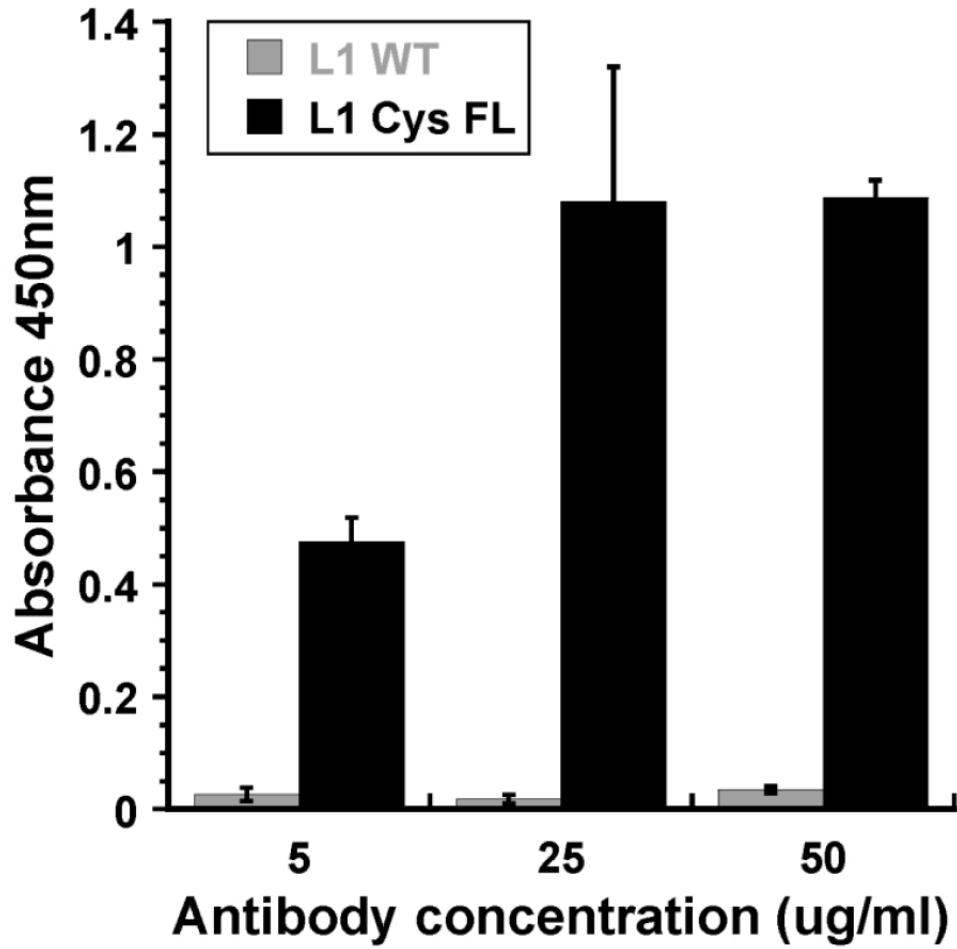
333  
334

335 **FIGURE 5** Transmission Electron Micrograph images of (a) assembled HPV16 L1-WT, (b) HPV16 L1-  
336 cysFL and (c) HPV18 L1-WT. Samples were air dried onto grid and stained with uranyl acetate. 50 nm  
337 scale bars are shown.



338  
339

340 **FIGURE 6** The DENV FL can be detected on assembled VLPs using a conformationally-sensitive human  
341 monoclonal Ab. Equalized quantities of assembled WT L1 and cysteine locked FL L1 VLPs were probed  
342 by ELISA using a conformationally-sensitive human monoclonal Ab against the fusion loop. This Ab  
343 specifically detected the FL containing chimeric VLPs, but did not react with the WT L1 VLPs.



344  
345

346 **REFERENCES**

- 347 1. Denis J, Majeau N, Acosta-Ramirez E, Savard C, Bedard M-C, Simard S, Lecours K, Bolduc  
348 M, Pare C, Willems B, et al. (2007) Immunogenicity of papaya mosaic virus-like particles fused  
349 to a hepatitis C virus epitope: Evidence for the critical function of multimerization. *Virology*  
350 [Internet] 363:59–68. Available from:  
351 <https://www.sciencedirect.com/science/article/pii/S004268220700027X>
- 352 2. Miura K, Stone WJR, Koolen KM, Deng B, Zhou L, van Gemert G-J, Locke E, Morin M,  
353 Bousema T, Sauerwein RW, et al. (2016) An inter-laboratory comparison of standard membrane-  
354 feeding assays for evaluation of malaria transmission-blocking vaccines. *Malar. J.* [Internet]  
355 15:463. Available from: [http://malariajournal.biomedcentral.com/articles/10.1186/s12936-016-](http://malariajournal.biomedcentral.com/articles/10.1186/s12936-016-1515-z)  
356 [1515-z](http://malariajournal.biomedcentral.com/articles/10.1186/s12936-016-1515-z)
- 357 3. Seitz H, Danthony T, Burkart F, Ottonello S, Müller M (2013) Influence of oxidation and  
358 multimerization on the immunogenicity of a thioredoxin-l2 prophylactic papillomavirus vaccine.  
359 *Clin. Vaccine Immunol.* [Internet] 20:1061–9. Available from:  
360 <http://www.ncbi.nlm.nih.gov/pubmed/23677323>
- 361 4. Yan M, Peng J, Jabbar IA, Liu X, Filgueira L, Frazer IH, Thomas R (2005) Activation of  
362 dendritic cells by human papillomavirus-like particles through TLR4 and NF- $\kappa$ B-mediated  
363 signalling, moderated by TGF- $\beta$ . *Immunol. Cell Biol.* [Internet] 83:83–91. Available from:  
364 <https://onlinelibrary.wiley.com/doi/10.1111/j.1440-1711.2004.01291.x>
- 365 5. Yu SS, Lau CM, Thomas SN, Jerome WG, Maron DJ, Dickerson JH, Hubbell JA, Giorgio TD  
366 (2012) Size- and charge-dependent non-specific uptake of PEGylated nanoparticles by  
367 macrophages. *Int. J. Nanomedicine* [Internet] 7:799. Available from:  
368 <http://www.ncbi.nlm.nih.gov/pubmed/22359457>
- 369 6. Victora GD, Nussenzweig MC (2012) Germinal Centers. *Annu. Rev. Immunol.* [Internet]  
370 30:429–457. Available from: [https://www.annualreviews.org/doi/10.1146/annurev-immunol-](https://www.annualreviews.org/doi/10.1146/annurev-immunol-020711-075032)  
371 [020711-075032](https://www.annualreviews.org/doi/10.1146/annurev-immunol-020711-075032)
- 372 7. Schiller JT, Lowy DR (1996) Papillomavirus-like particles and HPV vaccine development.  
373 *Semin. Cancer Biol.* [Internet] 7:373–382. Available from:  
374 <https://www.sciencedirect.com/science/article/abs/pii/S1044579X96900462>
- 375 8. Stanley M (2008) Immunobiology of HPV and HPV vaccines. *Gynecol. Oncol.* [Internet]  
376 109:S15–S21. Available from:  
377 [https://www.sciencedirect.com/science/article/pii/S0090825808001054?casa\\_token=eBt7UXG8](https://www.sciencedirect.com/science/article/pii/S0090825808001054?casa_token=eBt7UXG8qbQAAAAA:x4OVjWKwDiTUMGEPjv9Q4e3yoirjv5NM5nHBdSCZNpDp66KJk Wu68perYIIq6OYZ0gxzwJfjEA)  
378 [qbQAAAAA:x4OVjWKwDiTUMGEPjv9Q4e3yoirjv5NM5nHBdSCZNpDp66KJk Wu68perYII](https://www.sciencedirect.com/science/article/pii/S0090825808001054?casa_token=eBt7UXG8qbQAAAAA:x4OVjWKwDiTUMGEPjv9Q4e3yoirjv5NM5nHBdSCZNpDp66KJk Wu68perYIIq6OYZ0gxzwJfjEA)  
379 [q6OYZ0gxzwJfjEA](https://www.sciencedirect.com/science/article/pii/S0090825808001054?casa_token=eBt7UXG8qbQAAAAA:x4OVjWKwDiTUMGEPjv9Q4e3yoirjv5NM5nHBdSCZNpDp66KJk Wu68perYIIq6OYZ0gxzwJfjEA)
- 380 9. McLemore MR (2006) Gardasil®: Introducing the New Human Papillomavirus Vaccine. *Clin.*  
381 *J. Oncol. Nurs.* [Internet] 10:559–560. Available from: [http://cjon.ons.org/cjon/10/5/gardasil®-](http://cjon.ons.org/cjon/10/5/gardasil®-introducing-new-human-papillomavirus-vaccine)  
382 [introducing-new-human-papillomavirus-vaccine](http://cjon.ons.org/cjon/10/5/gardasil®-introducing-new-human-papillomavirus-vaccine)
- 383 10. Schellenbacher C, Roden R, Kirnbauer R (2009) Chimeric L1-L2 virus-like particles as  
384 potential broad-spectrum human papillomavirus vaccines. *J. Virol.* [Internet] 83:10085–95.  
385 Available from: <http://www.ncbi.nlm.nih.gov/pubmed/19640991>
- 386 11. Skolnick J, Kolinski A (1990) Dynamic Monte Carlo simulations of globular protein  
387 folding/unfolding pathways: I. Six-member, Greek key  $\beta$ -barrel proteins. *J. Mol. Biol.* [Internet]  
388 212:787–817. Available from:  
389 <https://www.sciencedirect.com/science/article/pii/002228369090237G>
- 390 12. Capaldi AP, Ferguson SJ, Radford SE (1999) The greek key protein apo-pseudoazurin folds  
391 through an obligate on-pathway intermediate. *J. Mol. Biol.* [Internet] 286:1621–1632. Available  
392 from:

393 [https://www.sciencedirect.com/science/article/pii/S0022283698925888?casa\\_token=FNz9e-](https://www.sciencedirect.com/science/article/pii/S0022283698925888?casa_token=FNz9e-)  
394 [KI2vkAAAAA:uEJmPvoA\\_ceR1DDhqzQ-o0RomNa6rOOUv-gnOrDgnpk73s2DBovOpCdr-](https://www.sciencedirect.com/science/article/pii/S0022283698925888?casa_token=FNz9e-KI2vkAAAAA:uEJmPvoA_ceR1DDhqzQ-o0RomNa6rOOUv-gnOrDgnpk73s2DBovOpCdr-)  
395 [yTWA0nRPe4NuGX55A](https://www.sciencedirect.com/science/article/pii/S0022283698925888?casa_token=FNz9e-yTWA0nRPe4NuGX55A)

396 13. Bork P, Holm L, Sander C (1994) The Immunoglobulin Fold: Structural Classification,  
397 Sequence Patterns and Common Core. *J. Mol. Biol.* [Internet] 242:309–320. Available from:  
398 <https://www.sciencedirect.com/science/article/pii/S0022283684715828>

399 14. Efimov A V. (1997) Structural trees for protein superfamilies. *Proteins Struct. Funct. Genet.*  
400 [Internet] 28:241–260. Available from: [https://onlinelibrary.wiley.com/doi/10.1002/\(SICI\)1097-](https://onlinelibrary.wiley.com/doi/10.1002/(SICI)1097-)  
401 [0134\(199706\)28:2%3C241::AID-PROT12%3E3.0.CO;2-I](https://onlinelibrary.wiley.com/doi/10.1002/(SICI)1097-0134(199706)28:2%3C241::AID-PROT12%3E3.0.CO;2-I)

402 15. Schellenbacher C, Roden R, Kirnbauer R (2009) Chimeric L1-L2 Virus-Like Particles as  
403 Potential Broad-Spectrum Human Papillomavirus Vaccines. *J. Virol.* 83:10085–10095.

404 16. Palatnik-de-Sousa CB, Soares I da S, Rosa DS (2018) Editorial: Epitope Discovery and  
405 Synthetic Vaccine Design. *Front. Immunol.* [Internet] 9:826. Available from:  
406 <http://journal.frontiersin.org/article/10.3389/fimmu.2018.00826/full>

407 17. Bente DA, Rico-Hesse R (2006) Models of dengue virus infection. *Drug Discov. Today Dis.*  
408 *Model.* [Internet] 3:97–103. Available from:  
409 [https://www.sciencedirect.com/science/article/pii/S1740675706000156?casa\\_token=ZKr3Hzk8F](https://www.sciencedirect.com/science/article/pii/S1740675706000156?casa_token=ZKr3Hzk8F)  
410 [kQAAAAA:eYGAZpjibV5oFllmq0Hh9Yvrn39DtcAq5gjOpc717HVqqJbZnsBbF9\\_c0NChns](https://www.sciencedirect.com/science/article/pii/S1740675706000156?casa_token=ZKr3Hzk8FkQAAAAA:eYGAZpjibV5oFllmq0Hh9Yvrn39DtcAq5gjOpc717HVqqJbZnsBbF9_c0NChns)  
411 [n-m1kH-3g](https://www.sciencedirect.com/science/article/pii/S1740675706000156?casa_token=ZKr3Hzk8Fn-m1kH-3g)

412 18. Bhatt S, Gething PW, Brady OJ, Messina JP, Farlow AW, Moyes CL, Drake JM, Brownstein  
413 JS, Hoen AG, Sankoh O, et al. (2013) The global distribution and burden of dengue. *Nature*  
414 [Internet] 496:504–507. Available from: <http://www.nature.com/articles/nature12060>

415 19. Halstead SB (2017) Dengvaxia sensitizes seronegatives to vaccine enhanced disease  
416 regardless of age. *Vaccine* [Internet] 35:6355–6358. Available from:  
417 [https://www.sciencedirect.com/science/article/pii/S0264410X17313610?casa\\_token=k22wjlk97](https://www.sciencedirect.com/science/article/pii/S0264410X17313610?casa_token=k22wjlk97)  
418 [nMAAAAA:ZSnG6bqGED1NSfAgghgx7G2\\_pHBbRNgXaUHR4aaEIV38WP-](https://www.sciencedirect.com/science/article/pii/S0264410X17313610?casa_token=k22wjlk97nMAAAAA:ZSnG6bqGED1NSfAgghgx7G2_pHBbRNgXaUHR4aaEIV38WP-)  
419 [25pxWInVQ0B9SgsE63ot-iBbBw](https://www.sciencedirect.com/science/article/pii/S0264410X17313610?casa_token=k22wjlk9725pxWInVQ0B9SgsE63ot-iBbBw)

420 20. Costin JM, Zaitseva E, Kahle KM, Nicholson CO, Rowe DK, Graham AS, Bazzone LE,  
421 Hogancamp G, Figueroa Sierra M, Fong RH, et al. (2013) Mechanistic Study of Broadly  
422 Neutralizing Human Monoclonal Antibodies against Dengue Virus That Target the Fusion Loop.  
423 *J. Virol.* [Internet] 87:52–66. Available from: <https://journals.asm.org/doi/10.1128/JVI.02273-12>

424 21. Schieffelin JS, Costin JM, Nicholson CO, Orgeron NM, Fontaine KA, Isern S, Michael SF,  
425 Robinson JE (2010) Neutralizing and non-neutralizing monoclonal antibodies against dengue  
426 virus E protein derived from a naturally infected patient. *Virol. J.* [Internet] 7:28. Available from:  
427 <https://virologyj.biomedcentral.com/articles/10.1186/1743-422X-7-28>

428 22. Huang CY-H, Butrapet S, Moss KJ, Childers T, Erb SM, Calvert AE, Silengo SJ, Kinney  
429 RM, Blair CD, Roehrig JT (2010) The dengue virus type 2 envelope protein fusion peptide is  
430 essential for membrane fusion. *Virology* [Internet] 396:305–315. Available from:  
431 <https://www.sciencedirect.com/science/article/pii/S0042682209006515>

432 23. Lu Z, Murray KS, Cleave V Van, LaVallie ER, Stahl ML, McCoy JM (1995) Expression of  
433 Thioredoxin Random Peptide Libraries on the Escherichia coli Cell Surface as Functional  
434 Fusions to Flagellin: A System Designed for Exploring Protein-Protein Interactions. *Nat.*  
435 *Biotechnol.* [Internet] 13:366–372. Available from:  
436 <http://www.nature.com/doi/10.1038/nbt0495-366>

437 24. Matsumura M, Signor G, Nature BM-, 1989 undefined Substantial increase of protein  
438 stability by multiple disulphide bonds. *nature.com* [Internet]. Available from:

439 [https://idp.nature.com/authorize/casa?redirect\\_uri=https://www.nature.com/articles/342291a0&c](https://idp.nature.com/authorize/casa?redirect_uri=https://www.nature.com/articles/342291a0&casa_token=4OdqHpl8xjAAAAAA:6D6gz33cPKKqgTNjY2NHlq5Ls_BcJhhai3dDwxzV37xIKC)  
440 [asa\\_token=4OdqHpl8xjAAAAAA:6D6gz33cPKKqgTNjY2NHlq5Ls\\_BcJhhai3dDwxzV37xIKC](https://idp.nature.com/authorize/casa?redirect_uri=https://www.nature.com/articles/342291a0&casa_token=4OdqHpl8xjAAAAAA:6D6gz33cPKKqgTNjY2NHlq5Ls_BcJhhai3dDwxzV37xIKC)  
441 [DJVhA3dILUuq-0wMImX4pFe9Ck9mKY4LwJ](https://idp.nature.com/authorize/casa?redirect_uri=https://www.nature.com/articles/342291a0&casa_token=4OdqHpl8xjAAAAAA:6D6gz33cPKKqgTNjY2NHlq5Ls_BcJhhai3dDwxzV37xIKC)  
442 25. Fersht AR (2000) Transition-state structure as a unifying basis in protein-folding  
443 mechanisms: contact order, chain topology, stability, and the extended nucleus mechanism. *Proc.*  
444 *Natl. Acad. Sci. U. S. A.* [Internet] 97:1525–9. Available from:  
445 <http://www.ncbi.nlm.nih.gov/pubmed/10677494>  
446 26. Okonechnikov K, Golosova O, Fursov M (2012) Unipro UGENE: a unified bioinformatics  
447 toolkit. *Bioinformatics* [Internet] 28:1166–1167. Available from:  
448 <https://academic.oup.com/bioinformatics/article-lookup/doi/10.1093/bioinformatics/bts091>  
449 27. Edgar RC (2004) MUSCLE: multiple sequence alignment with high accuracy and high  
450 throughput. *Nucleic Acids Res.* [Internet] 32:1792–7. Available from:  
451 <http://www.ncbi.nlm.nih.gov/pubmed/15034147>  
452 28. Buck CB, Pastrana D V., Lowy DR, Schiller JT Generation of HPV Pseudovirions Using  
453 Transfection and Their Use in Neutralization Assays. In: *Human Papillomaviruses*. New Jersey:  
454 Humana Press; 2005. pp. 445–462. Available from: [http://link.springer.com/10.1385/1-59259-](http://link.springer.com/10.1385/1-59259-982-6:445)  
455 [982-6:445](http://link.springer.com/10.1385/1-59259-982-6:445)  
456  
457